

GEODETIC MASS BALANCE OF THE PATAGONIAN ICEFIELDS DERIVED FROM SRTM AND TANDEM-X DATA

Wael Abdel Jaber¹, Dana Floricioiu¹ and Helmut Rott²

¹ German Aerospace Center (DLR) – IMF, Oberpfaffenhofen, Germany
² ENVEO IT, Innsbruck, Austria

ABSTRACT

We compare ice elevation from TanDEM-X Raw DEMs of summer 2014 and from the SRTM C-band DEM of summer 2000 over the Northern Patagonian Icefield (NPI) in order to obtain a detailed map of ice elevation change rates over the last 14 years. The geodetic method is used to compute the mass balance for this region and for the nearby Southern Patagonian Icefield (SPI). The method is outlined along with the error budget estimation. The backscattering coefficient of the data is analyzed in order to exclude elevation biases due to signal penetration in snow and firn.

Index Terms— TanDEM-X, elevation change maps, geodetic mass balance, Patagonian icefields

1. INTRODUCTION

The Northern and Southern Patagonian Icefields (NPI & SPI), represent the largest mid-latitude ice masses in the Southern Hemisphere. They are mostly drained by outlet glaciers with fronts calving into fresh water lakes or Pacific fjords. Both icefields were affected by significant downwasting in the last decades, as confirmed by low resolution mass trends obtained by inversion of GRACE derived satellite gravity fields [1]. Given their unique characteristics and the important contribution to sea level rise they represent a fundamental barometer for climate research. The Shuttle Radar Topography Mission (SRTM) of 2000 provided the most complete and accurate Digital Elevation Model (DEM) at the time covering the entire globe from 56°S to 60°N. The present TanDEM-X mission shares the same objective aiming at a global coverage with much higher resolution and accuracy. Their combination leads to a unique multitemporal elevation dataset based solely on SAR single pass bistatic interferometry characterized by 11 to 16 year time span: an ideal setup for monitoring long-term large-scale geophysical phenomena. Using this dataset, a detailed ice elevation change rate map was obtained for the ~13000 km² SPI [2] for the observation period 2000 - 2011/2012. In this paper we extend the same approach to the ~4000 km² NPI, and compute the mass balance for both icefields. The applied method along with the uncertainty estimation will also be outlined.

2. DATA

Both datasets used for this study are produced with bistatic single pass interferometry. This is the optimal configuration for DEM generation, not being affected by temporal decorrelation and fluctuations of atmospheric phase delay. The SRTM mission [3][4] was flown between 11 and 22 February 2000 on board the Space Shuttle Endeavour, equipped with a C-band and an X-band SAR bistatic interferometric systems. We rely on the C-band DEM, which has full coverage thanks to the wider 225-km swath. The final DEM product released by USGS was obtained by mosaicking and averaging all acquisitions falling within a 1°×1° tile. It subsequently underwent gap-filling and subsampling to 3 arcsec in its version 2.1, used here. Version 3.0 was recently released with full 1 arcsec resolution, along with swath image data (SRTMIMGR). This product contains the surface backscattering coefficient and the local incidence angle maps, which we used to interpret the conditions of the snow and firn, with the main objective of assessing possible signal penetration leading to an elevation bias. The low latitude of the SPI (48.3°S - 51.5°S) and NPI (46.4°S - 47.5°S) allowed the coverage with many ascending and descending passes, improving the relative accuracy of the SRTM DEM, which certainly exceeds for this region the nominal value of 16 m (90% linear point-to-point error) vertically and 15 m (90% circular error) horizontally.

The TanDEM-X mission [5] of the German Aerospace Center (DLR) was initiated in June 2010 with the objective of generating a truly global DEM with unprecedented accuracy. It is composed of two almost identical satellites flying in close helix formation, nominally operating their high resolution X-band SAR in bistatic mode. The operational Integrated TanDEM-X Processor (ITP) [6] was used to process carefully selected satellite raw datatakes over the NPI into Raw DEMs with full control over the whole processing chain. The length in azimuth of the scenes was adapted in order to maximize coverage of the icefield and to include flat ice-free (stable) terrain for calibration purposes (cf. Section 3). Additional supporting acquisitions were provided to perform multi baseline phase unwrapping [7], fundamental in regions of such complicated topography, featuring high mountains and intricate water bodies. The

height error map (HEM, indicating the interferometric error) and the calibrated amplitude (backscattering coefficient σ^0) image were also obtained from the ITP. The processed Raw DEMs, along with some parameters of their master acquisition, are listed in Table 1.

Table 1 – TanDEM-X Raw DEMs over NPI (all ascending).

ID	Date	h_{amb} [m]	θ [°]	Size [km]	Posting [arcsec]	PU type	Icefield coverage
N1	2014.02.14	50	34	30×119	0.4	MB	22.73%
N2	2014.01.01	68	37	30×133	0.4	MB	37.06%
N3	2014.01.01	68	37	30×133	0.2	SB	10.73%
N4	2014.01.12	68	37	30×133	0.4	MB	9.21%
N5	2013.09.02	64	36	30×133	0.2	SB	7.26%

3. METHODOLOGY

The first step to obtain the elevation change map consists in the accurate vertical and horizontal coregistration of DEMs. As argued in [8] this is a fundamental operation, a vertical offset between the DEMs affects equally all elevation difference samples. A horizontal shift causes a vertical error which is slope and aspect dependent. These errors are systematic, and would strongly affect the mass balance when integrated over large areas. The SRTM DEM (upscaled to 0.4 arcsec) was used as reference to coregister separately each TanDEM-X Raw DEM. This was done by manually selecting geographically distributed calibration regions (CR), which are used to assess the mean of the elevation difference between the SRTM and the TanDEM-X scene. The CR are chosen as flat and vegetation free as possible, to avoid coupling of vertical offset with height error caused by horizontal shift on slopes and to avoid differ penetration into canopy in X and C-band. By averaging all the CR mean Δh values, weighted by their standard error, a single elevation offset Δh_{reg} (and its uncertainty) is obtained for each Raw DEM. This is converted into a phase offset $\Delta\varphi_{reg} = (2\pi \cdot \Delta h_{reg})/h_{amb}$, which is fed into the ITP in order to re-geocode the Raw DEM, achieving a very precise calibration to the SRTM reference.

The single baseline TanDEM-X Raw DEMs led to better phase unwrapping results with 0.2 arcsec posting and were subsequently downsampled to 0.4 arcsec. Five elevation change rate maps (in $m a^{-1}$) have been obtained according to: $\frac{\Delta h}{\Delta t} = (h_{TDM} - h_{SRTM})/\Delta t$.

Due to the complicated topography some regions were still affected by phase unwrapping errors, particularly on the scenes processed with the single baseline procedure. These areas were selected on each Raw DEMs using thresholds on the elevation difference followed by manual editing and marked as invalid. To cover some of the gaps on the western margin of NPI, scene N5, acquired in September 2013, was added. Approximately 13% of the icefield surface remained unsurveyed with TanDEM-X data.

The $\Delta h/\Delta t$ images (without averaging), the Raw DEMs, the coherence, the HEM, and the σ^0 images were mosaicked with N1 in foreground and N5 in background (no averaging on overlapping regions).

In order to derive the mass balance, the mean elevation change rate $\langle \Delta h/\Delta t \rangle_b$ is computed across the entire icefield for altitude bins of 20 m, along with the icefield surface falling within that bin (*hypsoetry* or area-elevation distribution). The product of the two leads to the mean volume change rate per altitude bin. The values of $\langle \Delta h/\Delta t \rangle_b$ computed on the area covered by TanDEM-X are hence extrapolated to the unsurveyed area of the bin. The mass change rate curve is obtained multiplying by an ice density $\rho_i = 900 \pm 17 \text{ kg m}^{-3}$. Sorge's law is assumed to be valid implying that the vertical firm density profile is unchanged between the acquisitions. Finally, summing the contribution of all bins leads to the total volume and mass change rates.

4. BACKCATTERING ANALYSIS

Radar signal penetration in ice and snow causes the scattering phase center to be located below the actual surface, introducing an elevation bias in the InSAR DEM. On the glacier termini surface scattering is dominant because of their roughness, hence only the smoother plateau surface is susceptible of signal penetration. The penetration depth is linked to the dielectric properties of the snowpack, which are in turn strongly dependent on the liquid water content (LWC). Water causes a strong increase in absorption leading to a rapid fall of penetration depth. It also affects strongly the backscattering coefficient σ^0 , which can hence be used to interpret the snow condition.

An average σ^0 was obtained for all SRTM C-band acquisitions covering the plateau. The low radiometric accuracy (1 dB relative, 3 dB absolute), the ample range of look angles (30° - 59°) and the possibility of temporal changes in LWC during the 11 day mission introduce a certain uncertainty. The mean σ^0 was analyzed in conjunction with meteorological data collected by nearby stations. Temperatures were extended to the plateau by applying an appropriate lapse rate. Most of the plateau has low mean σ^0 (up to -28 dB) and low standard deviation, an indication of wet snow throughout the mission duration. This is expected since the acquisitions were done in summer. Some areas at higher altitude display higher σ^0 , here the upper snow layer might be refrozen but the lower layers still wet. This is supported by the temperature trend of the previous days (relatively warm) and the acquisition times (during night time). In both cases an elevation bias is likely negligible.

The TanDEM-X backscattering is obtained with very high radiometric accuracy. It was analyzed along with meteorological data, concluding that an InSAR elevation bias is unlikely on the whole NPI DEM mosaic.

As a side experiment a multiseasonal comparison of TanDEM-X elevation and σ^0 between the overlapping

winter scene N5 and the summer scene N3 (cf. Table 1) was performed. On a region of interest located on the plateau below 1350 m a low σ^0 of -19 dB, indicative of wet snow, is found in summer and on the relatively warm winter day of the N5 acquisition. Here a mean elevation difference $\Delta h = h_w - h_s = 1.8$ m is measured, likely due to the higher snow level during winter. Above 1350 m σ^0 drops to -10.5 in N5, indicating dry snow, and $\Delta h = -1.9$ m is measured on a confining region of interest. If the same seasonal elevation change is assumed for both regions, an elevation bias of approximately 3.7 m affects N5 where dry snow is present. These empirical estimations of seasonal change and penetration bias are used as rough references to model the error linked to these phenomena in the geodetic mass balance (cf. Section 5).

5. UNCERTAINTY ESTIMATION

An exhaustive explanation of the uncertainty of the mass balance exceeds the scope of this paper, hence only a brief outline of the included error sources and their estimation will be given here. The random error affecting each glacier elevation change rate sample $\Delta h/\Delta t$ was estimated empirically as the standard deviation of the ice-free $\Delta h/\Delta t$ with slope below 40° to better represent the icefield topography. The interferometric error depending on the coherence was found to be similar on and off-glacier.

From the random error of the $\Delta h/\Delta t$ samples the standard error of $\langle \Delta h/\Delta t \rangle_b$ is obtained by estimating the spatial correlation between adjacent samples through a semivariogram analysis, similarly to [9].

The vertical accuracy achieved coregistering each TanDEM-X Raw DEM to the SRTM DEM was treated as a systematic calibration error affecting equally all samples of the scene. The crustal uplift due to isostatic adjustments reported in [10] is considered mostly compensated by the calibration procedure.

The ideal acquisition period for mass balance computation is the end of the ablation season, around March for Patagonia. The NPI dataset was selected to meet as closely as possible this condition, being acquired in the same season as the SRTM DEM, both towards the end of the ablation season, minimizing at the same time risks of signal penetration in dry snow. The seasonal elevation bias caused by different acquisition season between the master and the slave DEM and their departure from the end of the ablation season was modeled together with the possible bias due to signal penetration in ice and snow. The two were included in the error budget as an independent source of systematic error.

The total error on $\langle \Delta h/\Delta t \rangle_b$ is arbitrarily doubled for the unsurveyed area of each altitude bin to account for its extrapolation.

Due to the lack of in-situ data, it was not possible to assess the validity of Sorge's law and estimate an uncertainty. A small error of 17 kg m^{-3} was assigned to the

ice density. Furthermore an error of 2% was assigned to the glacier area.

An elevation bias caused by the different resolution of the DEMs was not detected over the relatively gentle topography characterizing the icefield surface, confirming results found in the literature [11].

6. RESULTS

The detailed ice elevation change rate map obtained for NPI is shown in Figure 1. The glacier outline (marked by the black line) has been extracted from the Randolph Glacier Inventory (RGI) [12]. According to the latter the total glacier area is 3867.0 km^2 , of which an area of 3360.6 km^2 (87%) is covered by the TanDEM-X Raw DEMs (uncovered areas are shown in grey in Figure 1).

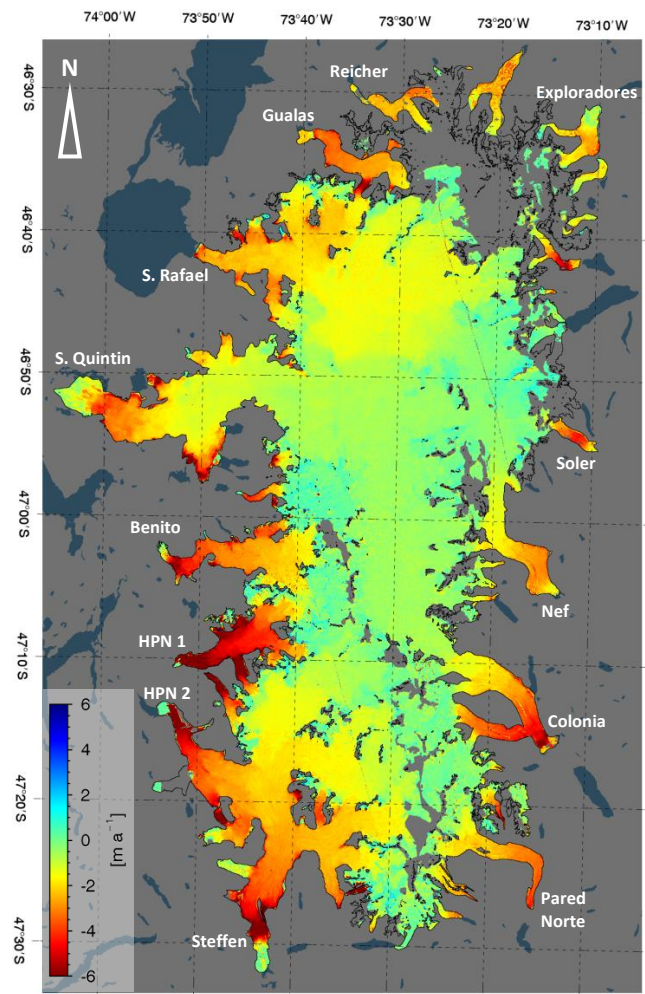


Figure 1 – Elevation change rate map of NPI for the observation period 2000 – 2014.

Although all glaciers of NPI display a thinning trend, its spatial pattern can vary significantly. Stronger thinning rates seem to affect the southwestern margin. Melting is relatively strong even on the plateau for glaciers such as HPN2,

Steffen and S. Rafael (-1.4 m a^{-1}), while it seems mostly concentrated on the termini for other glaciers (Benito, HPN1) characterized by a more abrupt elevation transition from plateau to terminus. The largest glacier, S. Quintin displays a thinning rate of -0.6 m a^{-1} on its plateau.

Table 2 – Mass balance results for NPI and SPI

Region	Area [km ²]	$\Delta V/\Delta t$ [km ³ a ⁻¹]	$\Delta M/\Delta t$ [Gt a ⁻¹]	$\Delta h/\Delta t$ [m w.e. a ⁻¹]	SLR [$\mu\text{m a}^{-1}$]
NPI	3867.0	-4.40 ± 0.13	-3.96 ± 0.14	-1.02 ± 0.04	10.94 ± 0.38
SPI	12880.7	-14.59 ± 0.37	-13.14 ± 0.42	-1.02 ± 0.03	36.29 ± 1.16

Table 2 summarizes the total mass balance of NPI between 2000 and 2014, obtained from the elevation change rate map in Figure 1 and the one of SPI obtained from the elevation change rates presented in [2] for the observation period 2000 – 2011/2012. The values do not include subaqueous ice loss, which have a limited impact on sea level change, although they have been estimated. Interestingly the mass balance per unit of area (mean $\Delta h/\Delta t$) is similar to for both icefields. The mass balance of these regions have also been obtained in [13] from SRTM and ASTER DEM data between 2000 and 2012. The authors report for NPI a total $\Delta V/\Delta t$ of $-4.9 \pm 0.3 \text{ km}^3 \cdot \text{a}^{-1}$ ($-1.23 \pm 0.08 \text{ m w.e. a}^{-1}$) which is higher of the one we obtain. They report for SPI a total $\Delta V/\Delta t$ of $-21.2 \pm 0.5 \text{ km}^3 \cdot \text{a}^{-1}$ ($-1.57 \pm 0.04 \text{ m w.e. a}^{-1}$) excluding subaqueous losses, a figure in disagreement with our result.

7. CONCLUSIONS

The strong potential offered by the combination of TanDEM-X and SRTM elevation data has been exploited to recover a detailed and accurate elevation change rate map of the NPI between 2000 and 2014. The strong variability of the melting pattern highlights the need of high resolution accurate elevation change maps for glaciological studies of such remote and inaccessible regions. The mass balance and the relative error budget have been computed through the geodetic method for the NPI and the much larger SPI. Our figures appear to be in contrast with results published in the literature, particularly over SPI.

8. REFERENCES

[1] T. Jacob, J. Wahr, T. W. Pfeffer and S. Swenson, "Recent contributions of glaciers and ice caps to sea level rise," *Nature*, vol. 482, pp. 514 - 518, 2012.

[2] W. Abdel Jaber, D. Floricioiu, H. Rott and M. Eineder, "Surface elevation changes of glaciers derived from SRTM and TanDEM-X DEM differences," in *IEEE IGARSS*, Melbourne, 2013.

[3] T. G. Farr, et al., "The Shuttle Radar Topography Mission", *Rev. Geophys.*, 45, RG2004, 2007.

[4] B. Rabus, M. Eineder, A. Roth, R. Bamler, "The shuttle radar topography mission- a new class of digital elevation models acquired by spaceborne radar", *Photogramm. Rem. Sens.*, v. 57, p. 241-262, 2003.

[5] G. Krieger, A. Moreira, H. Fiedler, I. Hajnsek, M. Werner, M. Younis and M. Zink, "TanDEM-X: A satellite formation for High-Resolution SAR Interferometry," *IEEE Transactions on Geoscience and Remote Sensing*, vol. 45, no. 11, pp. 3317 - 3341 , 2007.

[6] C. Rossi, F. Rodriguez G., T. Fritz, N. Yague-Martinez, M. Eineder, "TanDEM-X calibrated Raw DEM generation", *ISPRS Journal of Photogrammetry and Remote Sensing*, Vol. 73, pp. 12-20, 2012.

[7] M. Lachaise, T. Fritz, U. Bals and R. Bamler, "Phase unwrapping correction with dual-baseline data for the TanDEM-X mission," in *IEEE IGARSS*, Munich, 2012.

[8] C. Nuth and A. Käab, "Co-registration and bias corrections of satellite elevation data sets for quantifying glacier thickness change," *The Cryosphere*, vol. 5, no. 1, pp. 271-290, 2011.

[9] C. Rolstad, T. Haug, and B. Denby, "Spatially integrated geodetic glacier mass balance and its uncertainty based on geostatistical analysis: application to the western Svartisen ice cap," *Norway Journal of Glaciology*, International Glaciological Society, vol. 55, no. 192, pp. 666-680, 2009

[10] R. Dietrich, E. Ivins, G. Casassa, H. Lange, J. Wendt, and M. Fritsche, "Rapid crustal uplift in Patagonia due to enhanced ice loss," *Earth and Planetary Science Letters*, Elsevier, vol. 289, no. 1 pp. 22-29, 2010

[11] F. Paul, "Calculation of glacier elevation changes with SRTM: is there an elevation-dependent bias?" *Journal of Glaciology*, International Glaciological Society, vol. 54, no. 188, pp. 945-946, 2008

[12] A. Arendt, T. Bolch, J. G. Cogley, A. Gardner, J.-O. Hagen, R. Hock and G. Kaser, "Randolph glacier inventory v2.0: a dataset of global glacier outlines," Boulder, Colorado, USA, 2012.

[13] M. J. Willis, A. K. Melkonian, M. E. Pritchard and A. Rivera, "Ice loss from the Southern Patagonian Ice Field, South America, between 2000 and 2012," *Geophysical Research Letters*, vol. 39, no. L17501, 2012.

Acknowledgements

TanDEM-X data were provided within science proposal XTI_GLAC0495. Work supported by Helmholtz Alliance project Remote Sensing and Earth System Dynamics.